International Journal of Biological Macromolecules xxx (xxxx) 1–11

Contents lists available at ScienceDirect

International Journal of Biological Macromolecules

journal homepage: www.elsevier.com/locate/ijbiomac

Production of nanocellulose gels and films from invasive tree species

R.O. Almeida [a], A. Ramos [b], L. Alves [a], E. Potsi [a], P.J.T. Ferreira [a], M.G.V.S. Carvalho [a], M.G. Rasteiro [a], J.A.F. Gamelas [a,*]

[a] University of Coimbra, CIEPQPF, Department of Chemical Engineering, Pólo II, R. Sílvio Lima, PT – 3030-790 Coimbra, Portugal
[b] FibEnTech and Department of Chemistry, University of Beira Interior, PT - 6201-001 Covilhã, Portugal

ARTICLE INFO

Article history:
Received 20 April 2021
Received in revised form 21 July 2021
Accepted 3 August 2021

Keywords:
Cellulose nanofibrils
Circular economy
Waste valorisation
Inverse gas chromatography
Films
Invasive species

ABSTRACT

Wood/wastes from invasive tree species *Acacia dealbata* and *Ailanthus altissima* were used to produce high-value added nanocellulose. Firstly, bleached pulps were produced from the wood of these tree species after kraft cooking. Afterwards, the resultant pulps were pre-treated by TEMPO-mediated oxidation (*Acacia dealbata*) or enzymatic hydrolysis (*Ailanthus altissima*) followed by high-pressure homogenization. Hydrogels were obtained and characterized for their main physical and chemical properties, including rheology and evaluation of the surface properties of the freeze-dried materials by inverse gas chromatography. Results showed that micro/nanofibrils could be obtained from the wood of these invasive species. Rheometry studies showed that Acacia-TEMPO cellulose nanofibrils form strong gels with high yield stress point and viscosities (reaching ca. 100,000 Pa·s). Additionally, the surfaces of the obtained nanocelluloses showed a dispersive component of the surface energy near 40 mJ/m^2 and a prevalence of the Lewis acidic character over the basic one, as typical for cellulose-based materials. Finally, films with good mechanical and optical properties could be obtained from the cellulose hydrogels. *Acacia*-TEMPO film (produced by filtration/hot pressing) showed a tensile strength of 79 MPa, Young's modulus of 7.9 GPa, and a transparency of 88%. The water vapor barrier, however, was modest (permeability of 4.9×10^{-6} g/(Pa·day·m)).

1. Introduction

Invasive trees species can modify the chemical properties of the soil reducing the biodiversity, changing the ecological balance and affecting the native plant species [1,2]. *Acacia dealbata* and *Ailanthus Altissima* are considered to be two of the most aggressive and invasive species in Portugal, being distributed in all regions of Portugal [3]. *A. dealbata* is a particularly widespread, abundant, and problematic invader, native of Southeast Australia that has spread all over the world [2,3]. *A. dealbata* was introduced in Portugal for ornamental purposes, having been cultivated in the past as a forest species and for soil fixation. Its reproduction occurs through vigorous stump sprouts or root sprouts after cutting. It also reproduces by seminal way producing many seeds whose germination is stimulated by fire. *A. dealbata* has a significant impact on the ecosystem because it forms dense stands that compete with other species preventing their development (allelopathic properties), decreases the water lines flow and intensify erosion problems [3]. On the other hand, *A. dealbata* has several uses, specifically for the production of timber and tannins [4].

Ailanthus Altissima is native from China and has been introduced in many parts of the world. *A. altissima* is a medium-sized tree that reaches maximum heights of 18–30 m, and can grow up to 3 cm per day [5]. This species has prolific seed production, rapid juvenile growth, tolerance for harsh weather conditions and high levels of atmospheric pollution [6]. Each tree produces about 350,000 seeds per year that can travel long distances and germinate if there is adequate humidity [3]. It is used as an ornamental plant in urban areas, for roadside restoration and its biological properties and pharmacological applications have been extensively studied, being widely used in traditional Chinese medicine [6]. However, *A. altissima* has become a plague, by competing with native plants, and causing destruction on roads, sidewalks, structures, piping and orchards [5].

One way to control and valorise these invasive species may be to use them as raw material to produce high value-added products. These products may include lignin, cellulose, xylans, products from polysaccharide hydrolysis (sugars, furfural, hydroxymethylfurfural), bioethanol, etc. In the present work, the possibility of producing nanocellulose from *Acacia dealbata* and *Ailanthus Altissima* is considered. Nanocellulose is a fibrous material that can be obtained from cellulose and has at least one of its dimensions within the nanometer scale. Nanocellulose is a biodegradable nanomaterial with a large specific sur-

* Corresponding author.
E-mail address: jafgas@eq.uc.pt (J.A.F. Gamelas).

https://doi.org/10.1016/j.ijbiomac.2021.08.015
0141-8130/

face area, excellent mechanical properties, tailored crystallinity, and easy ability for surface functionalization. These singular properties allow it to have a variety of applications, e.g., energy devices, packaging, tissue engineering, nanocomposite materials, transparent paper with special functions, bio-medicine, etc. [7–9]. Nanocelluloses can be divided into three types: cellulose nanocrystals (CNCs), cellulose nanofibrils (CNFs) and bacterial cellulose (BC). All of these types of nanocelluloses are similar in their chemical composition. However, they have differences in morphology, particle size, crystallinity and in some other properties due to the difference of sources and production methods [7, 10]. CNCs are mainly produced by acid hydrolysis, using concentrated sulfuric acid, which typically degrades amorphous regions of cellulose and leaves intact the crystalline ones. BC is produced by bacteria (mainly by *Gluconacetobacter xylinum*) in aqueous culture media containing a sugar source. CNFs can be obtained from several wood or non-woody resources by using chemical (e.g., TEMPO-mediated oxidation or carboxymethylation) or enzymatic pre-treatments, followed by mechanical treatments (e.g., homogenization, ultrasonication) [10,11]. Depending on the extension of these treatments, fibrils at micro scale can also be obtained and thus the result is a mixture of micro- and nanocelluloses.

Some studies have already been conducted on the production of nanocelluloses from Acacia. Fall et al. [12] studied the influence of the wood species used on fiber wall disintegration: fibers from Eucalyptus, Acacia and Pine were enzymatically pre-treated and then mechanically fibrillated. The main results indicated that the degree of fibrillation seemed to be related to the charge density of the pristine fibers. The highest charged sample, the eucalyptus pulp, generated the highest degree of fibrillation. It was also found that the charge density of the micro/nanofibrils was higher than that of the original fibers. He et al. [13] worked in the mechanical fibrillation for the production of CNFs from chemical and mechanical pulps with different chemical compositions. They showed that the fibrillation of softwood pulp fibers from radiate pine was much faster and easier compared to hardwood pulp fibers from Acacia, due to the more rigid, complex, and heterogeneous structure of the hardwood fibers. Jasmani and Adman [14], prepared nanocrystalline cellulose (NCC) from *Acacia mangium* wood pulp via 64 wt% sulfuric acid hydrolysis. The acid hydrolysis was carried out on bleached pulp to produce NCC with a 79% crystallinity and an aspect ratio of 26. The resulting NCC was mixed with polyvinylalcohol (PVA) as a reinforcement material improving the tensile strength of the PVA film in 30% with only 2% of NCC. According to the authors, the NCC produced from Acacia has the potential to be used as a reinforcement material for composite applications. Finally, cellulose nanocrystals (CNCs) could be obtained from the exhausted bark of *Acacia mearnsii* (after industrial tannin extraction), following a sequence of delignification, bleaching and hydrolysis steps [15].

In the present work, wood/wastes from *Acacia dealbata* and *Ailanthus Altissima* were used for the production of nanocellulose. Following a previous kraft cooking and a bleaching sequence, whose processing conditions had to be optimized in each specific case in order to achieve target values of kappa number (cooking) and very low lignin content (bleaching), the resultant bleached pulps were submitted to a chemical or enzymatic pre-treatment, followed by high-pressure homogenization. The resultant nanocelluloses were extensively characterized for their physical and chemical properties, as well as for their surface properties by inverse gas chromatography. Films were also produced and characterized for their optical, structural, mechanical and water vapor barrier properties. The use of Ailanthus to produce nanocelluloses and related films has not yet been mentioned in the literature, which confers a novelty component to this work. Additionally, to our knowledge, this work is the first one to report the production of nanocellulose (gel and films) from Acacia by TEMPO-mediated oxidation.

2. Materials and methods

2.1. Bleached kraft pulps

Wood wastes from *Acacia dealbata* (branches) and *Ailanthus altissima* (trunk) were transformed into wood chips. The wood chips were cooked in a rotatory digester (Apineq) using a liquor-to-wood ratio of 3.5 (referred to a dry basis of wood) and a sulfidity of 28%. The digestor was heated from room temperature up to 160 °C at a heating rate of 1 °C/min and left at the maximum temperature for 60 min. Active alkali (AA) charges of 17% and 20% (based on Na_2O) were used for the cooking of *Ailanthus altissima* and *Acacia dealbata*, respectively. Then, the resultant pulps were submitted to a bleaching sequence ($D_0E_pD_1D_2$ for *A. dealbata* and $D_0E_pD_1$ for *A. altissima*, where D stands for chlorine dioxide and E_p for alkaline extraction reinforced with hydrogen peroxide) which allowed to obtain bleached pulps with an acceptable brightness (85–86% ISO) and a negligible Klason lignin content. The conditions used for the bleaching stages were: *A. dealbata*: D_0: 3.1% ClO_2 (as active chlorine on dry weight of pulp), 70 °C, 25 min; E_p: 1.6% NaOH, 0.4% H_2O_2, 80 °C, 90 min; D_1: 1% ClO_2, 70 °C, 180 min; D_2: 0.4% ClO_2, 75 °C, 90 min; *A. altissima*: D_0: 3.4% ClO_2, 70 °C, 25 min; E_p: 1.6% NaOH, 0.4% H_2O_2; 80 °C, 90 min, D_1: 1.2% ClO_2, 70 °C, 180 min. The bleached pulps were further refined at 4000 revolutions in a PFI beater, in order to make the fibrils more accessible.

In addition, the bleached kraft pulps were characterized for their sugars and lignin composition and for their intrinsic viscosity. The sugar content of the pulps was determined by high-performance liquid chromatography [16], using a Knauer instrument equipped with a refractive index (RI) detector and a Rezex ROA-Organic acid H column from Phenomenex. Lignin was determined following TAPPI T 222 and TAPPI UM 250 for the Klason and acid-soluble lignin, respectively. Intrinsic viscosity was determined based on ISO standard 5351.

2.2. CNF/CMF preparation

To produce the Acacia TEMPO-oxidised nanocellulose, the resulting kraft pulp was pre-treated with NaClO, NaBr and TEMPO (2,2,6,6-tetramethylpiperidine-1-oxyl radical) according to a general methodology described previously [17]. In short, 30 g (dry basis) of refined fibers was dispersed in distilled water containing TEMPO (0.016 g/g of fibers) and NaBr (0.1 g/g of fibers) at a consistency of 1%. Then, 80 mL of a NaClO solution (12.5% active chlorine) was added slowly to the previous mixture under constant mechanical stirring. After the oxidant addition, the reaction was left to run, being the pH of the medium kept at 10 by the constant addition of NaOH 0.1 M. The reaction was considered finished when the pH stabilized at 10 and no further addition of NaOH was required (after ca. 2 h). The oxidised fibers were then filtered and thoroughly washed with distilled water until the filtrate conductivity reached values comparable to that of distilled water. The fibers were then mechanically treated by high-pressure homogenization using two passes in the homogenizer (GEA Niro Soavi, model Panther NS 3006 L): first pass at ca. 600 bar and second pass at ca. 900 bar.

To produce the Ailanthus-Enzymatic nanocellulose, a commercial enzyme (endocellulase, 10% of exocellulase and 5% of hemicellulase) was used. The preparation of this material was carried out according to a methodology described elsewhere [18]. In short, the beaten fibers were suspended in water (3.5% consistency) and the pH was adjusted to 5 by the addition of sodium citrate buffer. The suspension was heated to 50 °C under constant mechanical stirring and the enzyme was added (300 g per ton of pulp). The cellulose hydrolysis was stopped after 2 h by heating the suspension to 80 °C for 15 min. The resulting suspension was cooled to room temperature and the fibers were filtered and washed with distilled water. The fibers were submitted to high-pressure homogenization, with a first pass at 500 bar and a second pass at 1000 bar.

2.3. CNF/CMF characterization

The final micro/nanofibrils were characterized for their solid content, fibrillation yield, carboxyl content (and the corresponding degree of substitution by carboxyl groups), intrinsic viscosity (from which the degree of polymerization was also estimated), zeta potential, size, and transparency. The procedures previously described for other CNFs from other sources were used [19,20] and are provided as supplementary material.

Field emission-SEM images were acquired for samples of the CNF/CMF (0.05% suspensions) previously deposited and air-dried on glass coverslips. The samples were sputter-coated with gold and analyzed in a Carl Zeiss Merlin microscope, in secondary electron mode. An acceleration voltage of 1 kV and working distance of 4.5 mm were used.

After freeze-drying, the crystallinity of the CNFs was also evaluated using X-ray diffraction. X-ray diffraction data were collected in a Bruker D8 ADVANCE diffractometer operating in the Bragg–Brentano configuration with Cu-Kα ($\lambda = 1.54$ Å) source at a current of 40 mA and an accelerating voltage of 40 kV. Data were collected by the step counting method (step 0.01° and time 0.5 s) in the 2θ range of 4–55°.

FTIR-ATR spectra of the freeze-dried CNFs were recorded using a Perkin Elmer spectrometer. Data were collected in the 500–4000 cm^{-1} range with a resolution of 4 cm^{-1} and 100 scans.

The inverse gas chromatography (IGC) analysis was performed using a DANI GC 1000 digital pressure control gas chromatograph equipped with a hydrogen flame ionization detector. Stainless-steel columns, 0.5 m long and 0.4 cm inside diameter were washed with acetone and dried before packing. For these analyses, 1.6 g and 2.3 g of nanocellulose (previously freeze-dried and softly milled in a coffee mill) were packed into the gas chromatograph column, for Acacia-TEMPO and Ailanthus-Enzymatic, respectively. The packed columns were shaped to fit the detector/injector geometry of the instrument, and, after that, were conditioned overnight at 105 °C, under a helium flow ($P = 0.05$ bar). Measurements were carried out at four different temperatures (35, 40, 45 and 50 °C) with injector and detector kept at 150 °C. Helium was used as the carrier gas. Small quantities of probe vapor (<1 μL) were injected into the carrier gas, allowing to work under infinite dilution conditions. The probes used for the IGC data collection were *n*-hexane (C6), *n*-heptane (C7), *n*-octane (C8), *n*-nonane (C9), *n*-decane (C10), trichloromethane (TCM, Lewis acidic probe), dichloromethane (DCM, acidic), tetrahydrofuran (THF, basic), diethyl ether (ether, basic), ethyl acetate (ETA, amphoteric), and acetone (amphoteric). The properties of these probes are listed in Table S1. The retention times were the average of three injections and were determined by the peak maximum for the *n*-alkanes, TCM and DCM and by the Conder and Young method for THF, ether, ETA and acetone, which provided less symmetrical chromatograms. The coefficient of variation between runs was typically lower than 5%. The theoretical aspects of IGC can be found in the literature [21–23]. In the present work, the dispersive component of the surface energy and the specific component of the work of adhesion of the distinct Lewis acid-base probes on the surface of the analyzed materials were obtained.

The rheological behavior of the Acacia-TEMPO suspension was also studied, due to the formation of a strong gel for the higher CNF concentrations. The mechanical rheometry was performed in a controlled stress rheometer (Haake, model RS1) using a cone-plate geometry (C60/1) for the rotational tests and a plate-plate geometry (PP20Ti) for the oscillatory tests, connected to a temperature control recirculation bath (Haake Phoenix II). Amplitude sweep tests were carried out at 0.1 Hz in the range of 0.1 to 100 Pa, and the flow curves were obtained in controlled stress mode applying shear stresses ranging between 0.1 and 100.0 Pa. Data were processed and analyzed using the Haake RheoWin 4.20.005 software.

2.4. Film production and characterization

CNF/CMF films were prepared by filtration followed by hot pressing. A filtration unit purchased from Kimble Ultra-ware Filtration systems and cellulose acetate membranes with 0.45 μm pore and 90 mm diameter supplied by Filtratech were used for the filtrations. After filtration, the films were dried at 110 °C for 10 min, using a pressure of ca. 2 N/cm^2, in a rapid dryer for laboratory sheets (Lorentzen & Wettre, model 257). With this method, it is possible to speed remarkably the production of the films and to obtain films with a high basis weight. Films were designed to have a basis weight up to 32–33 g/m^2.

The optical, structural and mechanical properties of the films were evaluated. Transparency was assessed on a Technidyne Color Touch 2 spectrophotometer. Measurements were performed on two replicate films using the illuminant D65 and the observer 10°. The transparency of the films was calculated according to the ISO 22891 standard. Basis weight was determined by the ratio between the mass and the area of the film. The thickness of the films was measured with a micrometer (Adamel Lhomargy, model MI 20) as the average of five specimens for each film. Tensile tests were performed at 23 °C and 50% RH using a tensile tester (Thwing-Albert Instrument Co., EJA series) according to ISO 1924/1 standard with the following changes: initial gap between grips was 5 cm and the tensile rate was 5 mm/min. The average of four specimens was taken for each film type. Tensile strength, Young's modulus, strain at rupture and breaking length were calculated.

Water vapor barrier properties were also measured for the films with higher basis weight. The water vapor transmission rate (WVTR) ($g/(m^2 \cdot day)$) and water vapor permeability (WVP) ($g/(Pa \cdot day \cdot m)$) were evaluated by gravimetric method according to the standard protocol ASTM E96-00. The films were fixed on the top of equilibrated cups containing a desiccant (15 g of anhydrous $CaCl_2$, dried at 105 °C before being used). The exposed film area was 29.22 cm^2. The test cups were then placed in a cabinet at 23 ± 1 °C and 50 ± 1% RH. The mass changes (Δm) were monitored every hour for 48 h. The WVTR was calculated by the ratio between the slope of the straight line (Δm/Δt) and the exposed film area in m^2. WVP was calculated according to the following equation.

$$WVP = \frac{WVTR}{\Delta P} \times e = \frac{WVTR}{P \times (RH_1 - RH_2)} \times e$$

where ΔP (Pa) is the difference in vapor pressure of water between both sides of the sample, P is the saturation vapor pressure at the test temperature, RH_1 and RH_2 are, respectively, the relative humidity of the cabinet (50%) and inside the cups (0%), and e is the thickness (m) of the films. The measurements were performed in duplicate.

3. Results and discussion

3.1. Bleached pulps from Acacia dealbata and Ailanthus altissima

The strategy developed for the production of nanocelluloses from the wood wastes of invasive tree species was based in the previous conversion of wood into pulps. Cooking and bleaching were required in order to obtain pulps with appropriate characteristics that would allow the production of nanocelluloses. For the cooking, the kraft process was applied, which is one of the most effective methods employed in the pulp industry to delignify wood without noticeably damaging the polysaccharide's structure. The target was to obtain pulps with kappa number of 15–16 (higher kappa would compromise the efficiency of the further bleaching step and lower kappa would be accompanied of too high cellulose depolymerization). For that, three cooking trials using *A. dealbata* were conducted at 160 °C for 1 h, using a sulfidity of 28% and alkali charges of 16, 20 and 24%. These conditions allowed producing pulps with kappa number of 19.7, 15.0 and 12.3, respectively. The *A. dealbata* pulp with kappa number of 15.0 and an intrinsic viscosity (a

measure of cellulose depolymerization) of 1241 cm^3/g was then selected for the following bleaching step. As for the cooking of *A. altissima*, two cooking trials were performed, using alkali charges of 17 and 24%. These allowed obtaining pulps with kappa number of 15.7 and 12.0, respectively. The pulp with kappa number of 15.7 and an intrinsic viscosity of 1189 cm^3/g was then used for the bleaching step.

The bleaching was based in a sequence of stages, employing charges of chlorine dioxide (D stage) and alkali with hydrogen peroxide (E_p stage). The objective was to obtain pulps with a very low lignin content. For *A. dealbata*, a sequence DE_pDD was applied, whereas for the bleaching of *A. altissima*, the bleaching was stopped after the second chlorine dioxide stage (DE_pD). An additional D stage was not applied in this case because the brightness achieved was similar to the one achieved for *A. dealbata* after the third D stage.

The most relevant characterization results of bleached pulps obtained from *A. dealbata* and *A. altissima* are summarized in Table 1. Results from other studies concerning bleached pulps are also presented for comparison.

The two bleached kraft pulps differed slightly in the chemical composition, with a higher cellulose content and a lower xylan content having been obtained for *A. altissima* pulp, similarly to the trend observed for the unbleached kraft pulps [24]. The total lignin content was practically the same and the Klason lignin was insignificant in both cases. Additionally, the chemical composition of the bleached kraft pulp produced from *A. dealbata* is comparable to the data obtained in other studies for other Acacia species [13,25]. The final values for the intrinsic viscosity of the bleached pulps indicated a reasonable high degree of cellulose polymerization.

3.2. Nanocelluloses from Acacia dealbata and Ailanthus altissima

After obtaining the bleached pulps, the possibility of their use in the production of nanocelluloses was evaluated. Two common approaches were selected: (1) TEMPO-mediated oxidation followed by high-pressure homogenization and (2) enzymatic pre-treatment followed by high-pressure homogenization. The characterization data of Acacia-TEMPO and Ailanthus-Enzymatic nanocelluloses produced from the bleached pulps are listed in Table 2.

As expected for the procedures used, the yield of nanofiber production was very high for Acacia-TEMPO (around 90%) and very low (near 10%) for Ailanthus-Enzymatic [19,20]. These yields were corroborated by the determinations of the degree of polymerization (DP), with a much higher DP observed for Ailanthus-Enzymatic than for Acacia-TEMPO, revealing the presence of longer fibers for enzymatic CMF. Moreover, even comparing with the bleached pulp used for its production (Table 1), the intrinsic viscosity of Ailanthus did not vary much after the enzymatic process (Table 2).

FE-SEM was used to study the fibril morphology and dimensions, as well to infer about the fibrillation state of the materials (Fig. 1). From the images obtained it was possible to observe that the nanofibers obtained from chemically pre-treated wood, Acacia-TEMPO, form a dense and continuous film, only revealing the shape of few long fibers which do not fibrillate. The high fibrillation degree obtained, allow the nanofibrils to arrange in the form of matted and continuous films, expected for materials at the nano-size. On the other hand, the images obtained for the material produced using enzymatic pre-treatment showed well defined nanofibrils with few microns in length and few nanometers (20–80 nm) in thickness mixed up with fibers of large dimensions. Besides, the nanosized fibrils were not fully exfoliated and separated from the large fibers during the pre-treatment and homogenization process, leading to a modest fibrillation yield.

The visible spectra in the transmittance mode (Fig. 2) also confirmed the higher amount of nanosized material for Acacia-TEMPO, which resulted in almost clear suspensions with a much higher transmittance than Ailanthus-Enzymatic. The determination of carboxyl groups showed a content five times higher for Acacia-TEMPO, with a degree of substitution of 0.14 and 0.03 for Acacia-TEMPO and Ailanthus-Enzymatic, respectively. Since the enzymatic process does not generate carboxyl groups, these come from the substituent glucuronic acid groups of xylan present in *Ailanthus altissima*. The quite different carboxyl content of these two nanocellulose samples was confirmed by FTIR-ATR (Fig. 3). In the highlighted area it can be seen a high-intensity band at 1603 cm^{-1} for Acacia-TEMPO, due to the CO stretching of the ionized COO^- groups. For Ailanthus-Enzymatic, this band was not clearly detected, indicating a very low content of carboxyl groups; in this case, only the OH bending vibration (1643 cm^{-1}) of water was observed. Accordingly, the zeta potential for Acacia-TEMPO was, as expected, more negative than that for Ailanthus-Enzymatic due to the higher abundance of carboxyl groups in Acacia-TEMPO nanocellulose structure. By using DLS, a comparison between the size (z average diameter) of the micro/nanofibrils obtained by the two methods was carried out. Acacia-TEMPO nanofibers were smaller, in accordance with the carboxyl content and the yield values obtained (Table 2). Since CMFs/CNFs are approximately cylindrical in shape and not spherical, the DLS has several limitations for the analysis of this type of materials. Besides, there is always a high polydispersity in the size distribution which adds difficulties in the analysis of the results. However, these re-

Table 1
Characterization data of bleached kraft pulps produced from *Acacia dealbata* and *Ailanthus altissima* woods.

	Present work		He et al. (2018)	Neto et al. (2004)
	A. dealbata	*A. altissima*	Acacia	*A. mangium*
Cellulose (%)	76.9 ± 0.2	80.6 ± 0.4	81.5	84.6
Xylan (%)	17.1 ± 0.1[a]	13.3 ± 0.0[a]	16.8	14.5
Klason lignin (%)	<0.1[b]	<0.1[b]	–	–
Acid-soluble lignin (%)	0.81 ± 0.05	0.72 ± 0.02	–	–
Total lignin (%)	~0.8	~0.7	0.8	0.5
Intrinsic viscosity (cm^3/g)	973 ± 2	935 ± 1	–	820
Brightness (ISO %)	85.6 ± 0.2	86.0 ± 0.1	–	90.7

[a] Acetyl groups and uronic acid groups are not included in the data.
[b] Below the sensitivity of the determination method.

Table 2
Characterization data of Acacia-TEMPO and Ailanthus-Enzymatic nanocelluloses.

Sample	Solid content (%)	Fibrillation yield (%)	Intrinsic viscosity (cm^3/g)	DP[a]	C_{COOH} (mmol/g)[b]	DS[c]	Transmittance[d] (600 nm, %)	Zeta potential (mV)	*Z*-Average (d, nm)
Acacia-TEMPO	0.71 ± 0.02	90.6 ± 1.6	142 ± 2	339	0.83 ± 0.01	0.14	64 ± 1	−76 ± 4	127 ± 30
Ailanthus-Enz	0.86 ± 0.03	8.9 ± 3.7	807 ± 11	2257	0.16 ± 0.04	0.03	10 ± 0	−42 ± 2	637 ± 78

[a] Degree of polymerization estimated from intrinsic viscosity measurements in cupriethylenediamine.
[b] Carboxyl group content.
[c] Degree of substitution by carboxyl groups.
[d] Transmittance for 0.1 wt% fibril suspensions.

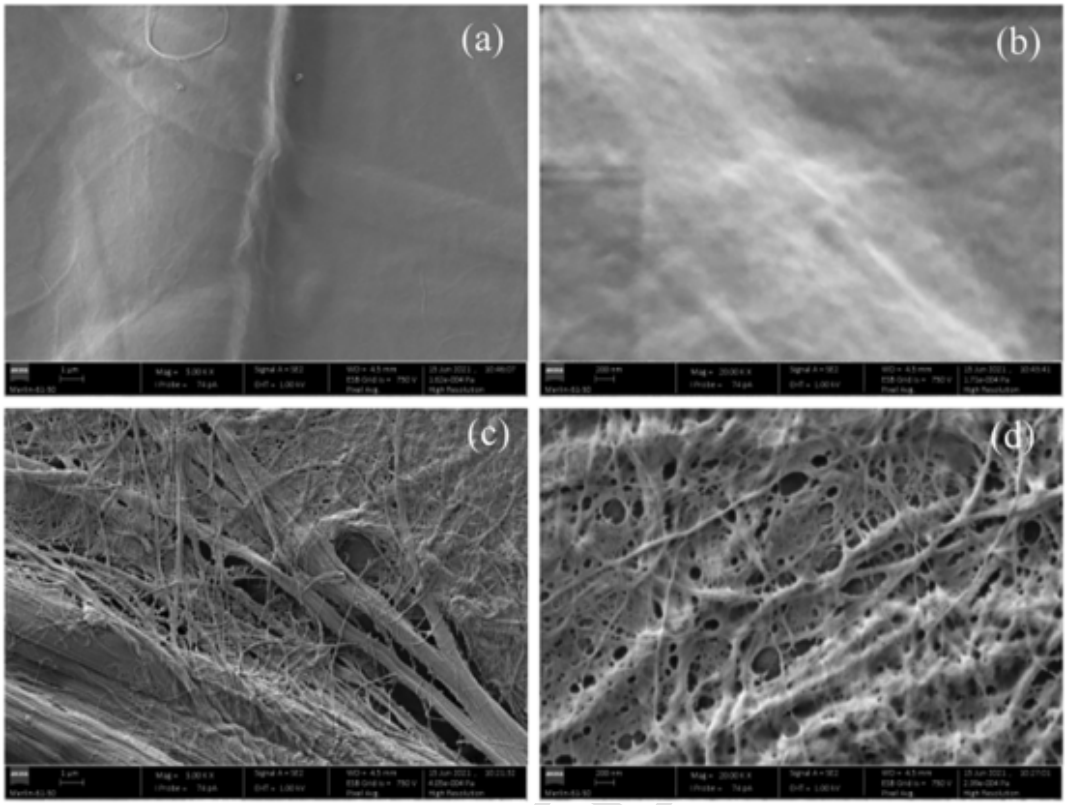

Fig. 1. FE-SEM images for Acacia-TEMPO (a and b) and Ailanthus-Enzymatic (c and d) at magnifications of 5000× (a and c) and 20,000× (b and d).

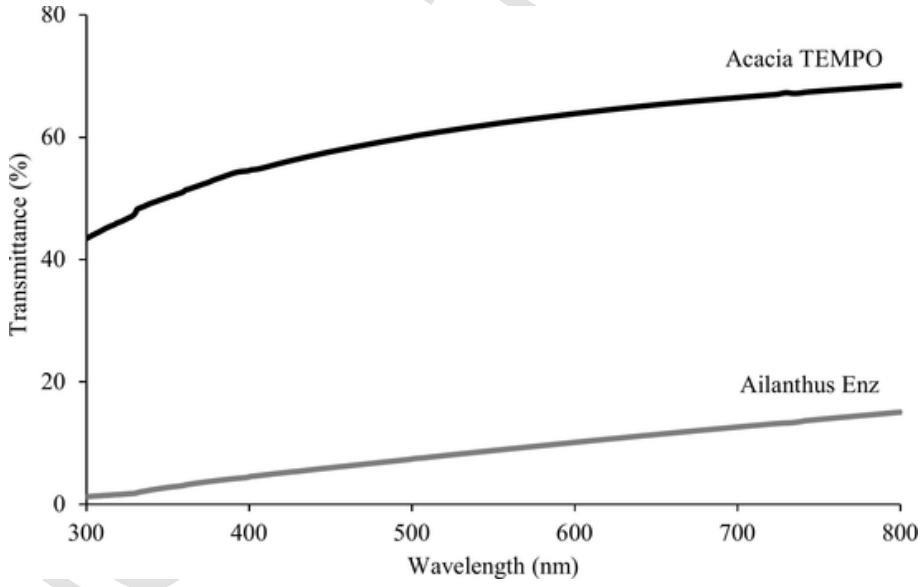

Fig. 2. Visible spectra in the transmittance mode of 0.1% suspensions of Acacia-TEMPO and Ailanthus-Enzymatic nanocelluloses.

sults provide important information about the size comparison of samples with similar structures [19].

Comparing these results for Ailanthus-Enzymatic with the data of Fall et al. [12], who prepared a nanocellulose from Acacia using an enzymatic process, several differences can be noted. Those authors obtained a material with a significantly lower intrinsic viscosity (336 cm^3/g; estimated DP of 721) and a higher nanofibrillation yield (32%). The unique very similar aspect was the zeta potential of the obtained material (−39 mV). Since the woods are not of the same origin this comparison can be biased. Additionally, it is known that the characteristics of enzymatic nanocelluloses, namely the DP, are much dependent on the type of enzyme used for their production [20]. The authors did not provide information about the carboxyl group content or the size of the fibers.

The nanofiber production (yield) and the degree of polymerization obtained for Acacia-TEMPO can also be compared with other results obtained for CNF from *Eucalyptus*. For instance, Lourenço and coworkers [26] produced a CNF by TEMPO-mediated oxidation from bleached *Eucalyptus globulus* kraft pulp with a carboxyl group content of 0.88 mmol/g, a nanofibrillation yield of 81%, an intrinsic viscosity of 164 cm^3/g (estimated DP of 390), and a zeta potential of −69 mV. These results are in general similar to those of the present study. How-

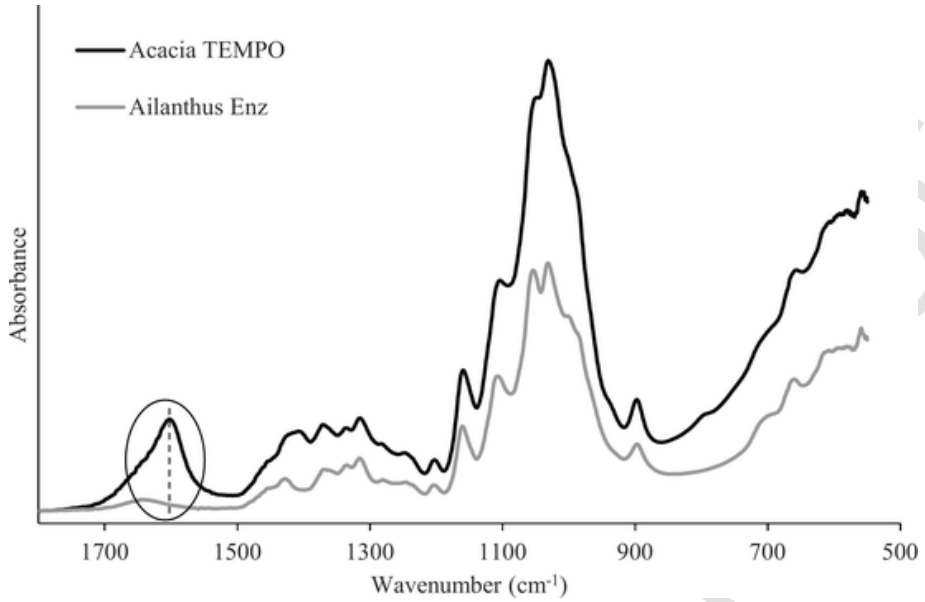

Fig. 3. FTIR-ATR spectra of Acacia-TEMPO and Ailanthus-Enzymatic nanocelluloses.

ever, in the present work, and for a similar carboxyl content, a higher nanofibrillation yield was apparently achieved using bleached *A. dealbata* fibers as the source of nanocellulose. Once again, the present results indicate that it is possible to produce CNFs from *A. dealbata* by TEMPO-mediated oxidation, having several similar properties to those obtained from *Eucalyptus* wood.

The rheological study performed with Acacia-TEMPO CNF suspension for different fibril concentrations is presented in Fig. 4: flow curves (top) and changes in phase angle (bottom). The apparent shear viscosity of the suspensions increased with the concentration, being observed a shear thinning behavior for all the samples, as expected for polymeric solutions; moreover, for concentrations above 0.18%, a typical pseudoplastic curve was observed, with the appearance of a yield stress point, which was shifted for higher stresses as the CNF concentration raises. Above a critical concentration (overlap concentration), the CNF suspensions form an entangled network, which is destroyed by an increase in the shear forces, leading to viscosity decrease. The estimated overlap concentration for the present CNF is between 0.12% and 0.18%, being observed a change in the flow curves profile between these two concentrations (Fig. 4, top) and detected a change from solid-like to liquid-like behavior (Fig. 4, bottom) for suspensions with 0.18% concentration and above, but not for the suspension with concentration below 0.18%. For the suspension containing 0.71% CNF, the viscosity at low shear values reached ca. 100,000 Pa·s and the yield stress point observed was ca. 35 Pa (flow curves) and 25 Pa (oscillatory sweep tests). The values obtained for the overlap concentration (formation of a gel for concentrations of at least 0.18%) and the viscosity values are similar to the values previously reported for TEMPO-CNF from Eucalyptus wood [27]. Therefore, the rheological study confirms the formation of a gel for suspensions containing above 0.18% of Acacia-TEMPO CNF, being the gel strength, the yield stress point and viscosity increased with concentration.

3.3. Analysis of the surface properties of nanocelluloses by inverse gas chromatography

The dispersive component of the surface energy (γ_s^d), and the specific component of the work of adhesion (W_a^s) of the polar probes evaluated, were determined. The results obtained at 35 °C for the two nanocelluloses are shown in Table 3 and in Fig. S1.

Regarding the γ_s^d parameter, a slightly higher value was obtained for Ailanthus-Enzymatic. However, these values are in the same range as those previously determined for other nanocellulose samples, obtained by similar processes, even if the wood species varies [29,30]. The effect of temperature on the dispersive component (γ_s^d) is presented in Fig. 5. For Ailanthus-Enzymatic a decreasing trend of the γ_s^d value with temperature in the range of studied temperatures (35–50 °C) was found, as reported for related cellulosic materials [30–32]. For Acacia-TEMPO, the γ_s^d variation with temperature was not as straightforward and differences between results at the different temperatures were very small. The maximum error in the determination of γ_s^d for cellulosic materials is typically 2 mJ m^{-2}. Thus, the differences between all studied temperatures for Acacia-TEMPO were within the range of the analysis error and the results inconclusive regarding the variation of γ_s^d with temperature. Additionally, the dispersive component of the surface energy was higher for Ailanthus-Enzymatic than for Acacia-TEMPO, for all investigated temperatures, although the values were closer for higher temperatures.

The results presented in Table 3 reveal that the nanocelluloses surfaces have a considerably higher affinity for Lewis amphoteric (ETA, acetone) and basic (THF, ether) probes than for acidic probes (TCM and DCM). The prevalence of the acidic surface character of the nanocelluloses is mainly due to the presence of acidic hydroxyl groups. Apparently, the adsorption of DCM in both nanocelluloses is not thermodynamically favored, since negative values for the W_a^s for this probe were obtained, which means that within the acidic probes, DCM is the one with the lowest affinity for the surface of the cellulose fibrils. The W_a^s(THF)/W_a^s(TCM) and W_a^s(ether)/W_a^s(TCM) ratios, that measure the prevalence of the Lewis acidity over the Lewis basicity of the material surface, decreased from Acacia-TEMPO to Ailanthus-Enzymatic. Acacia-TEMPO possesses a relatively high content of carboxyl groups (degree of substitution of approximately 0.14), mostly in the ionized form (COO^-) and not in protonated form (COOH), which could increase the Lewis basicity of the surface, reducing the ratio between basic and acidic probes. However, the opposite occurred, i.e., the mentioned ratios increased for Acacia-TEMPO, and this may be tentatively attributed to the higher exposure of the acidic hydroxyl groups in the surface of the more fibrillated CNF-TEMPO. The ionized form of the carboxylic acid groups was proved by the FTIR-ATR spectrum (Fig. 3), where the characteristic carboxylic acid (COOH) band at 1720–1730 cm^{-1} was not detected, and only the COO^- (ionized form) stretching band was observed. The W_a^s values, similarly to the γ_s^d parameter, were always

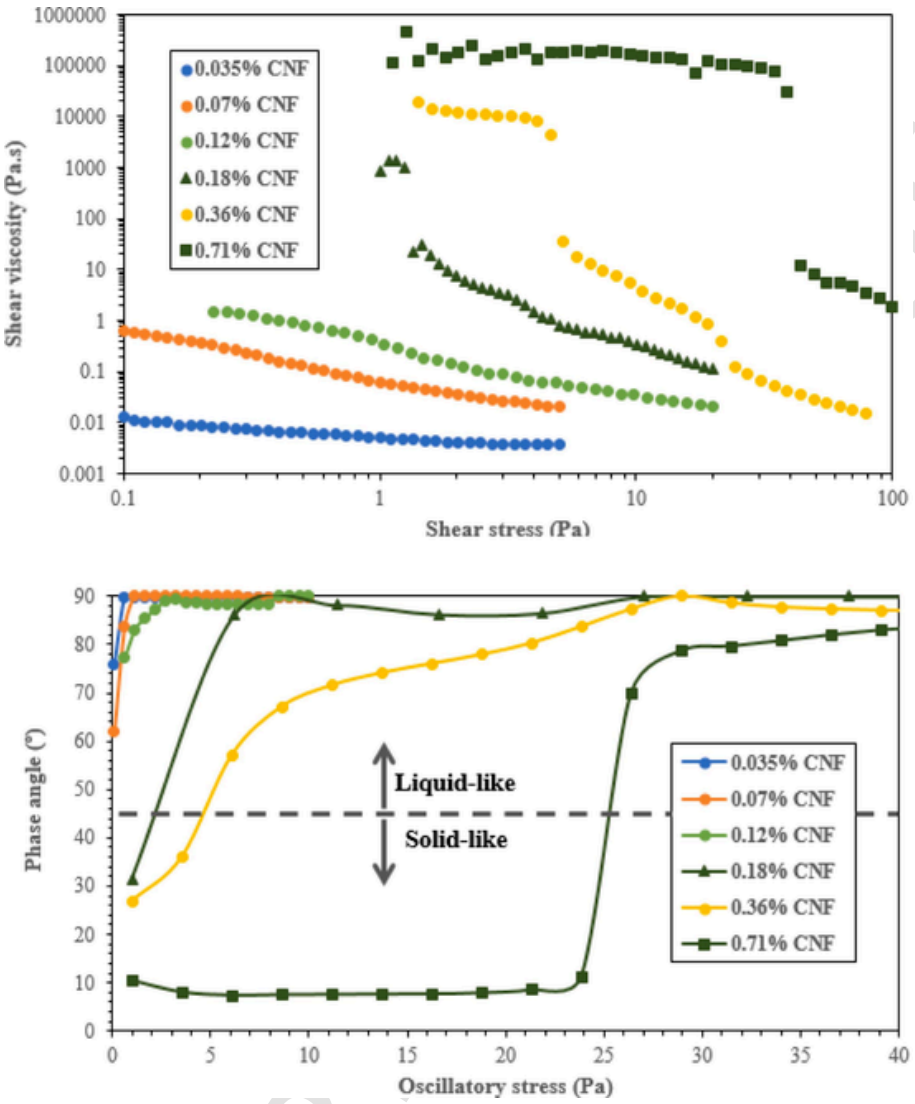

Fig. 4. Flow curves of Acacia-TEMPO CNF at different mass fractions (top); Changes in phase angle of Acacia-TEMPO CNF aqueous suspensions at different mass fractions, as function of oscillatory stress (at 0.1 Hz) (bottom). All the measurements were performed at 25 °C.

Table 3
Dispersive component of the surface energy (γ_s^d, mJ m^{-2}), and specific component of the work of adhesion (W_a^s, mJ m^{-2}) of polar probes for Acacia-TEMPO and Ailanthus-Enzymatic nanocelluloses[a].

Material	γ_s^d	W_a^s (TCM)	W_a^s (DCM)	W_a^s (THF)	W_a^s (Ether)	W_a^s (ETA)	W_a^s (Acetone)	W_a^s (THF)/W_a^s (TCM)	W_a^s (Ether)/W_a^s (TCM)
Acacia-TEMPO	38.3	2.8 ± 0.3	−6.0 ± 0.0	16.6 ± 0.5	13.7 ± 0.3	18.9 ± 0.6	25.0 ± 1.3	6.0	4.9
Ailanthus-Enz	42.6	4.3 ± 0.2	−2.3 ± 1.0	20.7 ± 0.4	17.2 ± 0.2	22.7 ± 0.0	28.5 ± 0.4	4.8	4.0

[a] Values (at 35 °C) calculated following Schultz and Lavielle approach [28].

higher for Ailanthus-Enzymatic than for Acacia-TEMPO. This trend was also observed previously by Gamelas et al. [30], using eucalypt wood to produce nanocelluloses. The higher γ_s^d and W_a^s values for Ailanthus-Enzymatic, could be tentatively explained as due to its higher crystallinity. Using X-ray diffraction (Fig. 6), the crystallinity index [33] was determined to be 80 and 63% for Ailanthus-Enzymatic and Acacia-TEMPO, respectively. As reported for this type of materials, more crystalline celluloses have higher surface energy and stronger intermolecular interactions, affording higher values of specific interactions with a wide range of probes [30,31].

To confirm the validity of the aforementioned statements, the specific interactions (W_a^s) at temperatures higher than 35 °C were also studied for these materials (Fig. 7). The W_a^s values of each probe were reasonably similar in the 35–50 °C range, except for TCM and DCM probes in Acacia-TEMPO. For the latter CNF, when increasing temperature from 35 to 40 °C to 45–50 °C, a significant decrease of the W_a^s (TCM) and W_a^s (DCM) values was observed. The acidic probes showed the lowest specific affinity among the tested probes for the surface of both the nanocelluloses, at all studied temperatures, and in Acacia-TEMPO this behavior was even more evident, especially at the higher temperatures of measurement. Overall, all the results of the specific interactions with Lewis acidic (TCM and DCM) and basic (THF and ether) probes, confirm that the two nanocelluloses have a more Lewis acidic than Lewis basic character. Additionally, acetone, an amphoteric probe, was clearly the one that showed the largest affinity with the surface of the CNFs/CMFs.

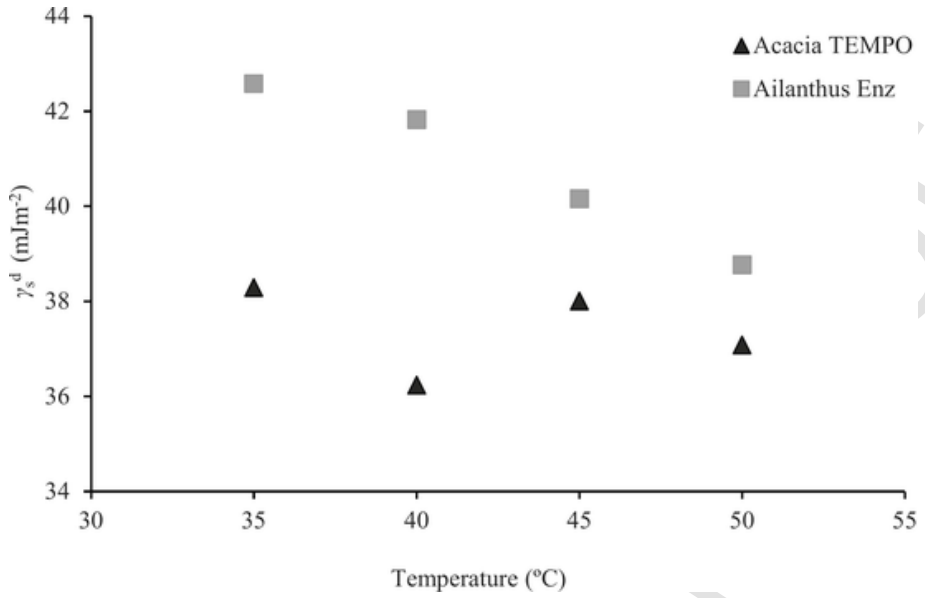

Fig. 5. γ_s^d values at several temperatures for Acacia-TEMPO and Ailanthus-Enzymatic nanocelluloses.

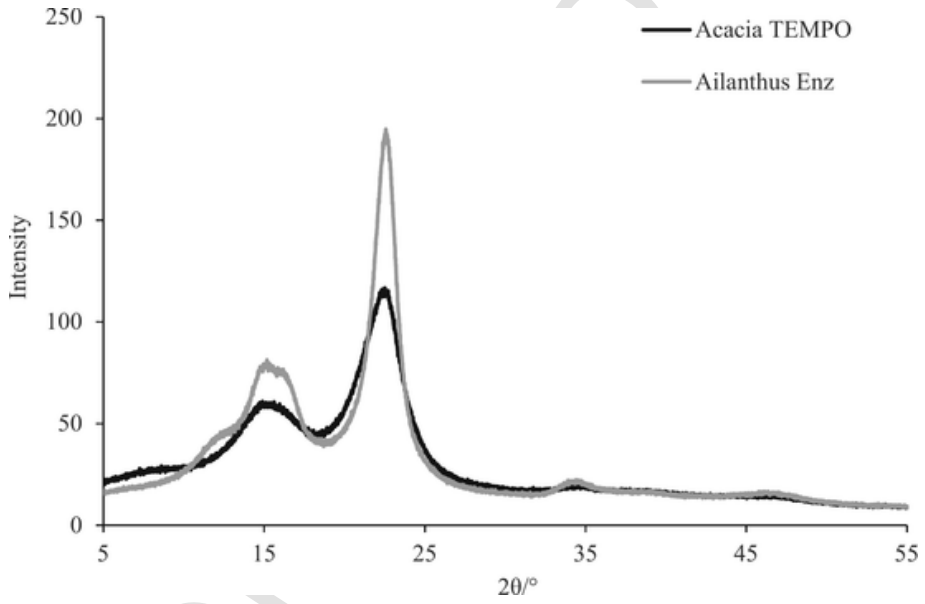

Fig. 6. X-ray diffractograms of Acacia-TEMPO and Ailanthus-Enzymatic nanocelluloses.

3.4. Film properties

Films of the two types of nanocellulose with different basis weight were produced by filtration followed by hot pressing. The results are presented in Table 4 and in Fig. 8. It is evident that films produced from nanocellulose obtained by TEMPO-mediated oxidation are significantly more transparent (transparency higher than 88%) than those produced from nanocellulose obtained by an enzymatic process. On the other hand, the thickness of the Ailanthus-Enzymatic films was higher than that of the Acacia-TEMPO films. This means that the shorter CNF-TEMPO nanofibers are able to conform themselves into a denser and more transparent film.

As for the strength properties, for each target basis weight, stronger (higher tensile strength) and stiffer (higher elastic modulus) films were obtained with Acacia-TEMPO, although with a lower strain at rupture. The more developed strength properties for the Acacia-TEMPO films can be related to the higher content of nanofibrils in this nanocellulose compared to Ailanthus-Enzymatic and the fact that they are more negatively charged. These are characteristics that may favor the strength properties of the films produced, as observed. Additionally, increasing the basis weight of the films produced by filtration/hot pressing seemed to promote some improvement in the overall tensile properties, particularly for Ailanthus-Enzymatic films.

The present results obtained for Acacia-TEMPO films are not far from those previously reported for films from eucalyptus nanofibrils. For instance, Rodionova et al. [34] produced films from eucalyptus nanofibrils obtained by TEMPO-mediated oxidation with different carboxyl content. The self-standing films were found to have tensile strength varying from about 10 MPa (carboxyl content of 0.4 mmol/g) up to near 65 MPa (carboxyl content of 1.2 mmol/g). The results obtained for Acacia-TEMPO of 67–79 MPa are thus comparable to the best results obtained by Rodionova [34]. Due to the brittleness of those eucalyptus TEMPO-CNF films, the authors could not measure the Young's modulus and therefore the values of this property cannot be compared.

Fall et al. [12] reported films from eucalyptus, acacia and pine using micro/nanofibrils produced by enzymatic pre-treatment with an en-

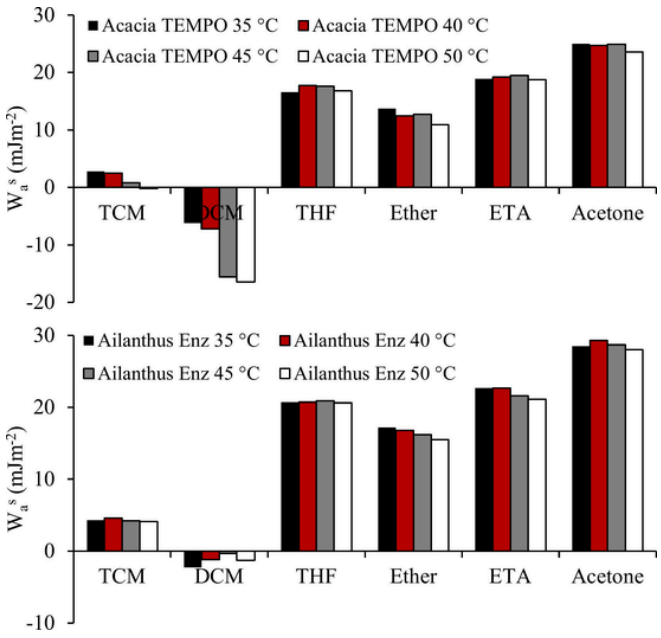

Fig. 7. Specific component of the work of adhesion (W_a^s) of several Lewis acid-base probes on the surface of Acacia-TEMPO and Ailanthus-Enzymatic nanocelluloses at 35–50 °C.

doglucanase. These films produced by vacuum filtration/hot drying presented values for the tensile strength, Young's modulus and strain at rupture in the range of 210–250 MPa, 9–10.5 GPa and 6.2–7.6%, respectively. The use of eucalyptus fibrils only slightly improved the strength properties in comparison to Acacia fibrils, and the authors related this increment with the higher fibrillation yield obtained for the eucalyptus micro/nanofibrils. The tensile strength and Young's modulus obtained in the present work for Ailanthus-Enzymatic are significantly lower, which could be largely related to the lower yield attained in the nanofibril production, of less than 10% (Table 2), whereas for the fibrils from the other sources, the corresponding yield reported in the literature was 30–49% [12]. In addition, the raw material is different and has a different composition in terms of polysaccharides (Table 1), which could affect the final strength values. The strain at rupture obtained for the film of higher basis weight of Ailanthus-Enzymatic was in a similar range to the results for eucalyptus, acacia and pine. Notwithstanding, even if the present results seem not to be as good as others found when using other tree species as raw materials to produce CNF/CMF films, they can still be considered as reasonable. Also, the conditions to produce the films were not optimized in the present work.

Gas barrier properties are also an important characteristic that films should have for their application in packaging or electronic devices. Although nanocellulose-based films are claimed to possess a good oxygen barrier, the barrier to water vapor is usually more limited, especially under high humidity conditions. WVTR and WVP of the films with higher basis weight were measured. The films presented WVTR values in the range of 150–250 g m^{-2} d^{-1} (Table 4), with lower values (better barrier) having been observed for the films of Ailanthus-Enzymatic. However, the water vapor permeability (WVP), which is a parameter that takes into account the thickness of the films, was lower for the films of Acacia-TEMPO (of similar basis weight), due to their lower thickness. The values of WVTR are in a similar range of those previously reported for instance for TEMPO-CNF films from wood of *Eucalyptus* and *Pinus radiata*: WVTR values of 285 and 292 g m^{-2} d^{-1} for films with thicknesses of 35 and 30 μm, respectively, were reported [35]. A film of neat cellulose nanofibrils produced from softwood presented a WVTR around 400 g m^{-2} d^{-1} [36]. The range of the obtained values indicate a relatively high hydrophilicity and water vapor permeability, which was somewhat predictable for films made of pure CMF/CNF. For a real application of this type of films obtained from wood wastes in gas barrier systems, even if they have a good oxygen barrier, other components will have to be added to impart water vapor barrier, e.g., clays [37]. Studies are being developed on this matter and the results will be presented in a future work.

4. Conclusions

Micro/nanofibrils were produced from the wood of *Acacia dealbata* and *Ailanthus altissima* invasive tree species using preliminary delignification processes, which had to be previously optimized, followed by chemical or enzymatic treatments and high-pressure homogenization. Acacia-TEMPO cellulose fibrils showed a large nanofibril content (fibrillation yield ~90%) and transparency. Based on rheology measurements, it was estimated that for concentrations of at least 0.18%, the Acacia-TEMPO CNF forms gels, whose strength increases with the CNF concentration. Ailanthus-Enzymatic showed a low fibrillation yield (around 10%) in account for the soft enzymatic process used for the pre-treatment of the cellulosic material, and, accordingly, transparency was remarkably lower.

The results from inverse gas chromatography analysis revealed that higher specific interactions were obtained with Lewis basic and Lewis amphoteric probes than with Lewis acidic probes, showing that the surfaces of the two nanocelluloses have a more Lewis acidic than Lewis basic character. However, for all the acid-base probes tested, higher specific interactions were obtained with Ailanthus-Enzymatic CMF, which was explained by the higher crystallinity of this sample compared with Acacia-TEMPO CNF.

Films produced from Acacia-TEMPO gel by filtration showed interesting optical and mechanical properties. In detail, the Acacia-TEMPO film showed a tensile strength of 79 MPa, Young's modulus of 7.9 GPa, and a transparency of 88%, which can be considered quite acceptable results. The results of water vapor permeability indicated a modest water vapor barrier (WVTR of 250 g m^{-2} d^{-1} and WVP of 4.9 × 10^{-6} g d^{-1} Pa^{-1} m^{-1}). The films from Ailanthus-Enzymatic showed worse optical properties (transparency of 53%) and a higher value for WVP.

Overall, the CNFs and CMFs produced from *A. dealbata* by TEMPO-oxidation and *A. altissima* by enzymatic process, respectively, have

Table 4
Optical, structural, mechanical and water vapor barrier properties of the films produced from Acacia-TEMPO and Ailanthus-Enzymatic nanocelluloses.

Film	Basis weight (g/m^2)	Transparency (%)	Thickness (μm)	Tensile strength (MPa)	Elastic modulus (MPa)	Strain at rupture (%)	WVTR (g m^{-2} d^{-1})[a]	WVP x 10^6 (g d^{-1} Pa^{-1} m^{-1})[a]
Acacia-TEMPO	18.9	88.4 ± 0.4	17 ± 2	67.3 ± 24.1	6035 ± 830	1.6 ± 1.1	–	–
Ailanthus-Enz	19.2	63.0 ± 0.6	38 ± 7	38.5 ± 3.4	3106 ± 225	3.0 ± 0.3	–	–
Acacia-TEMPO	32.8	88.0 ± 0.3	24 ± 1	78.7 ± 18.6	7924 ± 209	1.3 ± 0.6	250.1 ± 3.2	4.93 ± 0.44
Ailanthus-Enz	32.9	53.0 ± 3.3	46 ± 4	62.1 ± 1.7	3368 ± 136	6.7 ± 1.1	158.2 ± 8.7	6.38 ± 0.30

[a] WVTR refers to water vapor transmission rate and WVP to water vapor permeability.

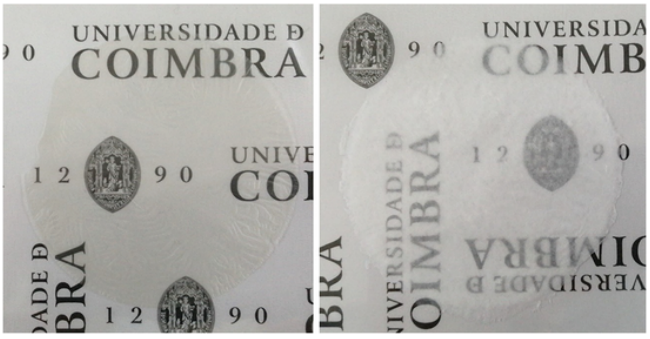

Fig. 8. Photographs of the films obtained through filtration + hot pressing from Acacia-TEMPO suspension (left) and Ailanthus-Enzymatic suspension (right).

many similarities with CNFs/CMFs produced from *Eucalyptus* wood, which allows to conclude that, indeed, the wastes of these invasive tree plants can be valorised towards the production of cellulose micro/nanofibrils, a product with increasingly high value-added, mitigating, at the same time, the problem of the tree proliferation in the natural systems. Wood/wastes of invasive species can be thus an alternative to more common woods to produce nanocellulose gels and nanocellulose films.

CRediT authorship contribution statement

Conceptualization: LA, PJTF, MGVSC, MGR, JAFG.
Methodology: AR, LA, MGVSC, JAFG.
Validation: RA, AR, LA, EP, MGVSC, JAFG.
Investigation: RA, AR, LA, EP, MGVSC, JAFG.
Writing - original draft: RA, JAFG.
Writing - review & editing: AR, LA, PJTF, MGVSC, MGR, JAFG.
Supervision: PJTF, MGVSC, MGR, JAFG.
Project administration: MGR, JAFG.
Funding acquisition: MGR, JAFG.

Acknowledgments

Authors thank the support from project MATIS (2020 000014 MATIS 2020) funded by Agência para o Desenvolvimento e Coesão (Portugal). The RAIZ – Instituto de Investigação da Floresta e do Papel and the FCT through Strategic Research Centre Project (UIDB/00102/2020) are also acknowledged.

Appendix A. Supplementary data

Supplementary data to this article can be found online at https://doi.org/10.1016/j.ijbiomac.2021.08.015.

References

[1] N.R. Jordan, D.L. Larson, S.C. Huerd, Soil modification by invasive plants: effects on native and invasive species of mixed-grass prairies, Biol. Invasions 10 (2008) 177–190, https://doi.org/10.1007/s10530-007-9121-1.
[2] L. Lazzaro, C. Giuliani, A. Fabiani, A.E. Agnelli, R. Pastorelli, A. Lagomarsino, R. Benesperi, R. Calamassi, B. Foggi, Soil and plant changing after invasion: the case of Acacia dealbata in a Mediterranean ecosystem, Sci. Total Environ. 497–498 (2014) 491–498, https://doi.org/10.1016/j.scitotenv.2014.08.014.
[3] H. Marchante, E. Marchante, H. Freitas (Eds.), Plantas invasoras em Portugal – fichas para identificação e controlo, Coimbra, 2005.
[4] A.J. Gouws, C.M. Shackleton, Abundance and correlates of the Acacia dealbata invasion in the northern eastern cape, South Africa, For. Ecol. Manag. 432 (2019) 455–466, https://doi.org/10.1016/j.foreco.2018.09.048.
[5] P. Baptista, A.P. Costa, R. Simões, M.E. Amaral, Ailanthus altissima: an alternative fiber source for papermaking, Ind. Crop. Prod. 52 (2014) 32–37, https://doi.org/10.1016/j.indcrop.2013.10.008.
[6] G.A. Walker, M. Gaertner, M.P. Robertson, D.M. Richardson, The prognosis for Ailanthus altissima (Simaroubaceae; tree of heaven) as an invasive species in South Africa; insights from its performance elsewhere in the world, S. Afr. J. Bot. 112 (2017) 283–289, https://doi.org/10.1016/j.sajb.2017.06.007.
[7] P. Phanthong, P. Reubroycharoen, X. Hao, G. Xu, A. Abudula, G. Guan, Nanocellulose: extraction and application, Carbon Resour. Convers. 1 (2018) 32–43, https://doi.org/10.1016/j.crcon.2018.05.004.
[8] Z. Fang, G. Hou, C. Chen, L. Hu, Nanocellulose-based films and their emerging applications, Curr. Opin. Solid State Mater. Sci. 23 (2019) 100764, https://doi.org/10.1016/j.cossms.2019.07.003.
[9] P. Thomas, T. Duolikun, N.P. Rumjit, S. Moosavi, C.W. Lai, M.R.B. Johan, L.B. Fen, Comprehensive review on nanocellulose: recent developments, challenges and future prospects, J. Mech. Behav. Biomed. Mater. 110 (2020) 103884, https://doi.org/10.1016/j.jmbbm.2020.103884.
[10] T. Abitbol, A. Rivkin, Y. Cao, Y. Nevo, E. Abraham, T. Ben-Shalom, S. Lapidot, O. Shoseyov, Nanocellulose, a tiny fiber with huge applications, Curr. Opin. Biotechnol. 39 (2016) 76–88, https://doi.org/10.1016/j.copbio.2016.01.002.
[11] O. Nechyporchuk, M.N. Belgacem, J. Bras, Production of cellulose nanofibrils: a review of recent advances, Ind. Crop. Prod. 93 (2016) 2–25, https://doi.org/10.1016/j.indcrop.2016.02.016.
[12] A.B. Fall, A. Burman, L. Wågberg, Cellulosic nanofibrils form eucalyptus, acacia and pine fibers, Nord. Pulp Paper Res. J. 29 (2014) 176–184, https://doi.org/10.3183/npprj-2014-29-01-p176-184.
[13] M. He, G. Yang, J. Chen, X. Ji, Q. Wang, Production and characterization of cellulose nanofibrils from different chemical and mechanical pulps, J. Wood Chem. Technol. 38 (2018) 149–158, https://doi.org/10.1080/02773813.2017.1411368.
[14] L. Jasmani, S. Adnan, Preparation and characterization of nanocrystalline cellulose from Acacia mangium and its reinforcement potential, Carbohydr. Polym. 161 (2017) 166–171, https://doi.org/10.1016/j.carbpol.2016.12.061.
[15] T. Taflick, L.A. Schwendler, S.M.L. Rosa, C.I.D. Bica, S.M.B. Nachtigall, Cellulose nanocrystals from acacia bark–Influence of solvent extraction, Int. J. Biol. Macromol. 101 (2017) 553–561, https://doi.org/10.1016/j.ijbiomac.2017.03.076.
[16] P.J.T. Ferreira, J.A.F. Gamelas, M.G.V.S. Carvalho, G.V. Duarte, J.M.P.I. Canhoto, R. Passas, Evaluation of the papermaking potential of Ailanthus altissima, Ind. Crop. Prod. 42 (2013) 538–542, https://doi.org/10.1016/j.indcrop.2012.06.030.
[17] T. Saito, S. Kimura, Y. Nishiyama, A. Isogai, Cellulose nanofibers prepared by TEMPO-mediated oxidation of native cellulose, Biomacromolecules 8 (2007) 2485–2491, https://doi.org/10.1021/bm0703970.
[18] Q. Tarrés, E. Saguer, M.A. Pèlach, M. Alcalà, M. Delgado-Aguilar, P. Mutjé, The feasibility of incorporating cellulose micro/nanofibers in papermaking processes: the relevance of enzymatic hydrolysis, Cellulose 23 (2016) 1433–1445, https://doi.org/10.1007/s10570-016-0889-y.
[19] A.F. Lourenço, J.A.F. Gamelas, T. Nunes, J. Amaral, P. Mutjé, P.J. Ferreira, Influence of TEMPO-oxidised cellulose nanofibrils on the properties of filler-containing papers, Cellulose 24 (2017) 349–362, https://doi.org/10.1007/s10570-016-1121-9.
[20] A.F. Lourenço, J.A.F. Gamelas, P. Sarmento, P.J.T. Ferreira, Enzymatic nanocellulose in papermaking – the key role as filler flocculant and strengthening agent, Carbohydr. Polym. 224 (2019) 115200, https://doi.org/10.1016/j.carbpol.2019.115200.
[21] P. Mukhopadhyay, H.P. Schreiber, Aspects of acid-base interactions and use of inverse gas chromatography, Colloids Surf. A Physicochem. Eng. Asp. 100 (1995) 47–71, https://doi.org/10.1016/0927-7757(95)03137-3.
[22] J.M.R.C.A. Santos, J.T. Guthrie, Analysis of interactions in multicomponent polymeric systems: the key-role of inverse gas chromatography, Mater. Sci. Eng. R 50 (2005) 79–107, https://doi.org/10.1016/j.mser.2005.07.003.
[23] J.A.F. Gamelas, The surface properties of cellulose and lignocellulosic materials assessed by inverse gas chromatography: a review, Cellulose 20 (2013) 2675–2693, https://doi.org/10.1007/s10570-013-0066-5.
[24] R. Almeida, F. Cisneros, C.V.T. Mendes, M.G.V.S. Carvalho, M.G. Rasteiro, J.A.F. Gamelas, Valorisation of invasive plant species in the production of polyelectrolytes, Ind. Crop. Prod. 167 (2021) 113476, https://doi.org/10.1016/j.indcrop.2021.113476.
[25] C.P. Neto, A.J.D. Silvestre, D.V. Evtuguin, C.S.R. Freire, P.C.R. Pinto, A.S. Santiago, Bulk and surface composition of ECF bleached hardwood kraft pulp fibers, Nord. Pulp Paper Res. J. 19 (2004) 513–520, https://doi.org/10.3183/npprj-2004-19-04-p513-520.
[26] A.F. Lourenço, J.A.F. Gamelas, P. Sarmento, P.J.T. Ferreira, Cellulose micro and nanofibrils as coating agent for improved printability in office papers, Cellulose 27 (2020) 6001–6010, https://doi.org/10.1007/s10570-020-03184-9.
[27] L. Alves, E. Ferraz, A.F. Lourenço, P.J. Ferreira, M.G. Rasteiro, J.A.F. Gamelas, Tuning rheology and aggregation behavior of TEMPO-oxidised cellulose nanofibrils aqueous suspensions by addition of different acids, Carbohydr. Polym. 237 (2020) 116109, https://doi.org/10.1016/j.carbpol.2020.116109.
[28] J. Schultz, L. Lavielle, C. Martin, The role of the Interface in carbon fibre-epoxy composites, J. Adhes. 23 (1987) 45–60, https://doi.org/10.1080/00218468708080469.
[29] N. Siddiqui, R.H. Mills, D.J. Gardner, D. Bousfield, Production and characterization of cellulose nanofibers from wood pulp, J. Adhes. Sci. Technol. 25 (2011) 709–721, https://doi.org/10.1163/016942410x525975.
[30] J.A.F. Gamelas, J. Pedrosa, A.F. Lourenco, P.J. Ferreira, Surface properties of distinct nanofibrillated celluloses assessed by inverse gas chromatography, Colloids Surf. A Physicochem. Eng. Asp. 469 (2015) 36–41, https://doi.org/10.1016/j.colsurfa.2014.12.058.
[31] E. Papirer, E. Brendle, H. Balard, C. Vergelati, Inverse gas chromatography investigation of the surface properties of cellulose, J. Adhes. Sci. Technol. 14 (2000) 321–337, https://doi.org/10.1163/156856100742627.
[32] M.G. Carvalho, J.M.R.C.A. Santos, A.A. Martins, M.M. Figueiredo, The effects of

beating, web forming and sizing on the surface energy of Eucalyptus globulus Kraft fibers evaluated by inverse gas chromatography, Cellulose 12 (2005) 371–383, https://doi.org/10.1007/s10570-004-7738-0.

[33] L. Segal, J.J. Creely, A.E. Martin, C.M. Conrad, An empirical method for estimating the degree of crystallinity of native cellulose using X-ray diffractometer, Textile Res. J. 29 (1959) 786–794, https://doi.org/10.1177/004051755902901003.

[34] G. Rodionova, T. Saito, M. Lenes, O. Eriksen, O. Gregersen, H. Fukuzumi, A. Isogai, Mechanical and oxygen barrier properties of films prepared from fibrillated dispersions of TEMPO-oxidized Norway spruce and eucalyptus pulps, Cellulose 19 (2012) 705–711, https://doi.org/10.1007/s10570-012-9664-x.

[35] C. Honorato, V. Kumar, J. Liu, H. Koivula, C. Xu, M. Toivakka, Transparent nanocellulose-pigment composite films, J. Mater. Sci. 50 (2015) 7343–7352, https://doi.org/10.1007/s10853-015-9291-7.

[36] A.H. Tayeb, M. Tajvidi, Sustainable barrier system via self-assembly of colloidal montmorillonite and cross-linking resins on nanocellulose interfaces, ACS Appl. Mater. Interfaces 11 (2019) 1604–1615, https://doi.org/10.1021/acsami.8b16659.

[37] L. Alves, E. Ferraz, J.A.F. Gamelas, Composites of nanofibrillated cellulose with clay minerals: a review, Adv. Colloid Interf. Sci. 272 (2019) 101994, https://doi.org/10.1016/j.cis.2019.101994.